E-Journal of Advanced Maintenance Vol.7-2 (2015) 179-188
Japan Society of Maintenology

Equivalent current models and the analysis of directional ECT signals

Weiying CHENG[1,*]

1 *NDE Center, Japan Power Engineering and Inspection* Corporation, *14-1, Benten-cho, Tsurumi-ku, Yokohama 230-0044, Japan*

ABSTRACT

Eddy current testing was studied from both the 'transmission' and 'receiving' sides. The distributions of eddy current and magnetic field were analyzed, and the defect-induced eddy current perturbation was modeled by equivalent current models, permitting qualitative interpretation of each directional magnetic field signals. Investigation also showed that the signals resulting from the bypassing of eddy currents under a crack are appropriate for depth sizing and that from the bypassing to a crack's longitudinal ends are appropriate for length sizing. The accuracy of defect sizing can be improved by using the combination of multi-directional magnetic field signals.

KEYWORDS

eddy current testing, magnetic field, equivalent current model, sizing, cracks

ARTICLE INFORMATION

Article history:
Received 26 December 2014
Accepted 24 July 2015

1. Introduction

Eddy current testing (ECT) is extensively used for material characterization, defect detection, and etc [1]. The ECT signals are required to be highly sensitive to the parameters subject to measurement, while insusceptible to other unwanted factors. For example, an ECT probe to measure the thickness of a non-metallic coating should be sensitive to liftoff variation, whereas a probe to detect defects is not. Regarding the assessment of a defect's depth and/or length, signals most pertinent to depth and/or length should be utilized. Overall, an ECT probe's detectability and sizing ability are to be evaluated with regard to the parameters subject to inspection.

In the studies to enhance the detection and sizing abilities of ECT, several models have been proposed to provide qualitative interpretation of defect-field patterns and to design probes to improve the responses from particular defects. L.Atherton proposed an anomalous source defect model [2], in which the eddy currents diving under a non-penetrating slit were modeled by a solenoid source current and the eddy currents driven around the ends of a slit were modeled by anomalous current whorls. The current whorl model is applicable to a crack's longitudinal ends but not the central part. In order to overcome this insignificancy, an elliptical loop model is proposed in this study so that the eddy currents bypassing laterally of a crack can be analyzed in full length.

In addition, magnetic fields perpendicular to a pickup coil's surface are measured in conventional ECT. The perpendicular-to-pickup coil field component is not always most appropriate for particular ECT purpose. In this study, vectorial magnetic field signals are analyzed by the proposed models and the respective directional field components' sizing abilities are evaluated, permitting optimum arrangement of excitation and pickup coil/sensors. Eddy current testing experiments are carried out to take multi-directional field component signals. And the depth sizing abilities of the respective directional signals are verified.

2. Eddy currents and magnetic fields of a defect-free specimen

A typical drive-pickup mode ECT probe consists of excitation coils to induce eddy currents and pickup coils/sensors to acquire magnetic flux density signals. Excitation coils are generally either

* Corresponding Author, E-mail: cheng-weiying@japeic.or.jp

perpendicular (vertical) or parallel (horizontal) to a specimen. If the specimen is assumed to be perpendicular to the **Z**-axis, the axis of a vertical coil is in the **Z** direction, and that of a horizontal coil is normal to the **Z**-axis.

Fig. 1 shows a circular-shaped vertical coil, the eddy currents it induces, and the magnetic field lines. Above the coil center, the magnetic field's **Z** component, **Bz**, is of maximum magnitude, while the **X** and **Y** components are 0. With a pickup sensor positioned at the excitation coil's axis to take the **Bz** signals, the probe is sensitive to the variations of liftoff and/or the specimen's electro-magnetic properties. However, if the pickup sensor over there is oriented otherwise to take the **X** or **Y** directional fields, the probe would be insusceptible to liftoff variation and of high S/N ratio for defect detection.

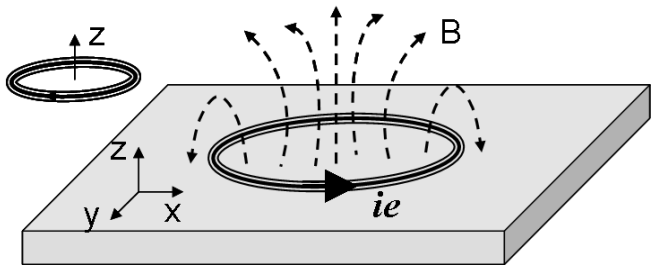

Fig. 1 A vertical coil and eddy currents, magnetic field lines.

Similar analysis was applicable to rectangular-shaped horizontal coils. Fig. 2 shows that eddy currents are in the excitation coil's wiring direction (**Y** direction in Fig. 2), and the magnetic field lines are parallel to the coil's axis (X direction in Fig. 2). Beneath the excitation coil, the **X** directional magnetic field component, **Bx**, is of maximum magnitude, whereas the **Z** and **Y** components are 0. Therefore, with a magnetic field sensor right below the center of the horizontal excitation coil, the probe is sensitive to liftoff variation if the sensor is oriented to take the **X** directional component, whereas be insensitive to liftoff variation if the pickup sensor is oriented to take the **Z** or **Y** directional components.

The above-mentioned analysis shows that the sensitivity of ECT should be considered in respect of the configurations of excitation coils and pickup sensors.

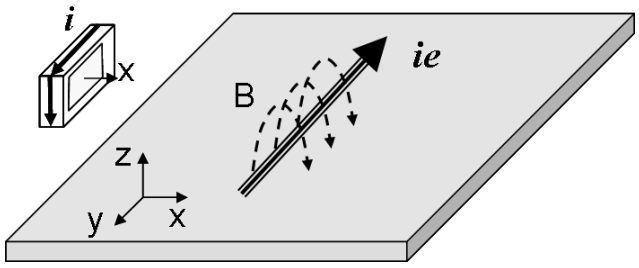

Fig. 2 A typical horizontal coil, the eddy current and magnetic field lines.

3. Defect-induced eddy currents and the equivalent current models

In the presence of a defect, eddy currents change their flow by bypassing laterally around and under the defect. The change of eddy currents can be approximated by subtracting the eddy currents of a cracked specimen from that of a crack-free specimen. In the present study, the perturbation of eddy currents and magnetic field signals were analyzed with respect to the vertical and horizontal excitation coils, respectively. It is to be noticed that 'crack' in the undermentioned analysis is assumed to be planar and rectangular-shaped, that is, of same depth in a crack's longitudinal direction.

3.1. Vertical excitation coil and the perturbation of defect-induced eddy currents

In this sub-section, the circular-shaped vertical coil shown in Fig. 1 was utilized and magnetic flux density signals ('signal' hereafter) were taken by a pickup sensor installed at the center of the excitation coil.

3.1.1. Eddy currents dive beneath a crack

Fig. 3 shows that eddy currents induced by the circular-shaped excitation coil diverted under a crack can be modeled by two solenoid coils: when the probe is right above the crack center, the two solenoid coils are exactly alike but with reversed currents (Fig.3(a)), and the **Bx** signal received by the centrally located pickup sensor is 0; when the probe moves away from the crack center in the longitudinal direction, the two solenoid coils and the reversed currents are no longer the same (Fig. 3(b)), so that the **Bx** signal is nonzero. When the probe approaches the longitudinal ends of a crack, the two solenoid coils merge into one, and **Bx** is of largest magnitude. The **Bx** signals are anti-symmetric about crack center.

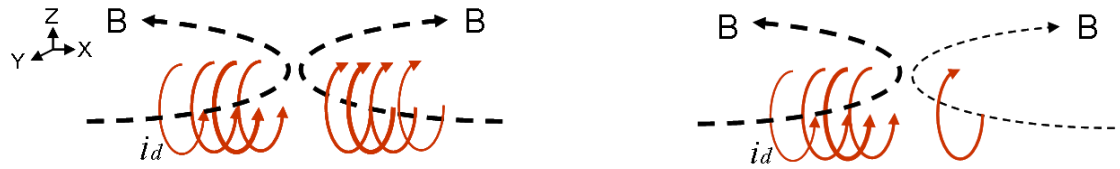

Fig. 3 Solenoid coil model and magnetic flux lines.

3.1.2. Eddy currents bypass laterally around a crack

The change of eddy currents caused by bypassing to a crack's side surfaces can be modeled by elliptical current loops as depicted in Fig. 4. When the probe is right above the crack center, signal **Bz** is largest and the other directional signals are 0. However, when the probe moves away from the crack center, currents in the hypothetical elliptical loop decrease, in addition, the sensing point misaligns with the elliptical loop's central point, signal **Bz** decreases consequently.

When the probe moves longitudinally over a crack, the perpendicular-to-the-crack signal, **By,** is always 0. However, when the probe deviates from the right-above-the-crack scan path, the center of the hypothetical elliptical loop deviates from the sensor, **By** is nonzero. **By** signals on the two sides of a crack are anti-symmetric. The magnitude of the **By** signal is determined by the eddy current density, the distance between the hypothetical loop and the pickup sensor, and the dimension of the elliptical loop. Because the dimension of the elliptical loop is pertinent to the length of a crack, **By** signal is considered to be appropriate for length sizing.

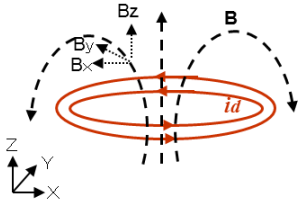

Fig. 4 Elliptical loop current model and magnetic flux lines.

3.1.3. Verification of the equivalent current models: **Bx** and **By** signals measured by a GMR sensor probe

The analysis in sections 3.1.1 and 3.1.2 was verified by a GMR sensor-embedded ECT probe consisting of a circular-shaped excitation coil (inner diameter 8mm, outer diameter 14mm, thickness 10mm) and a centrally installed GMR sensor (NVEAA004-02) whose sensing direction is on the excitation coil's surface (Fig. 5). The probe can receive longitudinally directional signals if the GMR sensor's sensitive axis is parallel to the crack (Fig. 5). By the way, by rotating the probe 90 degrees, perpendicular-to-the-crack signals can be measured.

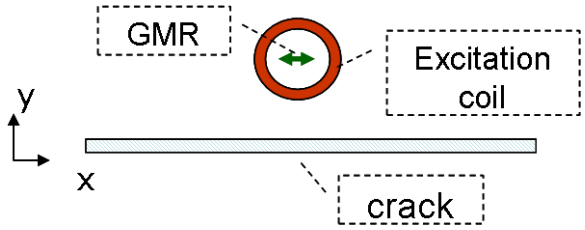

Fig. 5 A GMR sensor embedded probe and crack.

Fig. 6 shows the **Bx** signals of a 30 mm long, 0.2mm wide, 1.5 mm deep slit acquired by the GMR sensor probe (by Multiscan5800, at 10 kHz). Fig. 6(a) shows C-scan signals over a 60mm X 35mm area, and Fig. 6(b) shows the signals taken along a right-above-the-crack path. The **Bx** signal is 0 when the probe is just above crack center, of largest magnitude in the vicinity of the crack's longitudinal ends, and the signals are 180 degrees out of phase with respect to the crack center.

The GMR sensor's sensitive direction is perpendicular to the crack if the probe is 90 degrees rotated (Fig. 7). Fig. 7 shows the **By** signal is zero right over the crack, increases when the probe moves away from the crack, reaches peak magnitude when the probe is at a certain distance from the crack, and decreases when the probe moves further away. The **By** signals on the two sides of the crack are antisymmetric.

The measurement signals behaved consistent with the equivalent solenoid coil and elliptical loop models based analysis, showing effectiveness of the equivalent current models.

3.1.4. Directional ECT signals and the dimension of a crack

Although the crack induced eddy current perturbation could be decomposed into bypasses under and laterally of a crack and modeled respectively by equivalent solenoid coil and elliptical current loop models, the magnetic field signals are the effects of diversions in all directions. Under the excitation of a circular-shaped vertical coil, it is considered that

- Since the **Bx** signals are mainly resulted from the bypassing of eddy currents under a crack, **Bx** signal should be more relevant to crack depth.
- The **Bz** and **By** signals are mainly due to the laterally diversion of eddy currents and therefore should be more relevant to crack length.

Cracks of various depths (1, 2, 4, 7, and 9mm) but fixed length (30mm) and width (0.2mm) were assumed in the center of a 10mm thick and sufficiently large test piece whose conductivity and relative permeability are respectively 1MS/m and 1. The GMR sensor probe was assumed to scan longitudinally right above the cracks with 1mm liftoff. The excitation frequency was 20kHz and the skin depth under this condition was 3.56mm (calculated by $1/\sqrt{\pi f \mu \sigma}$)

The **Bx** and **Bz** signals were calculated by finite element method (FEM) numerical simulation. By respectively setting the maximum amplitudes of **Bx** and **Bz** signals of the 1mm deep (30mm long, 0.2mm wide) slit as 1, the maximum amplitudes of signals of other slits were calibrated accordingly. The relation between crack depth and respective signals' magnitudes is presented in Fig. 8, in which the skin depth is noted as Δ and the crack depth is indicated by Depth/Δ. It is observed that both the **Bx** and **Bz** signals increase with crack depth and tend to saturate at certain depth. However, the **Bx** signal is less likely to saturate with crack depth than **Bz**. This agrees with the analysis that the signal mainly resulted from the bypassing of eddy currents under a crack is more pertinent to crack depth.

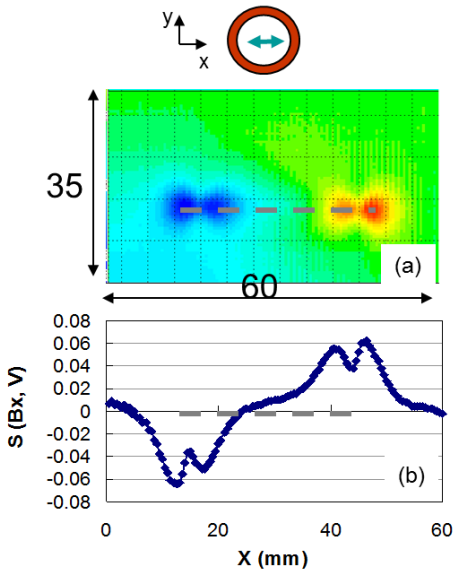

Fig. 6 The Bx signal of a 30mm long, 0.2mm wide, 1.5mm deep slit, measured by GMR sensor probe. (a) the C-Scan of the Bx signal, (b) signal taken along a over-the-crack scan path. The gray dashed line indicates the location of the crack.

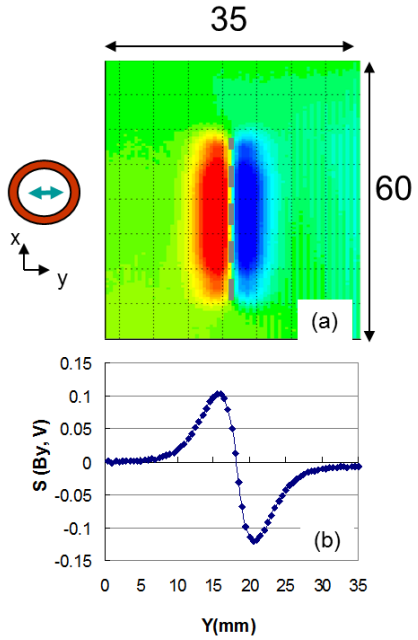

Fig.7 the By signal of a 30mm long, 1.5mm deep slit, measured by GMR sensor probe. (a) Cscan of the By signal, (b) signal taken above the vertical centerline. The gray dashed line indicates the location of the crack.

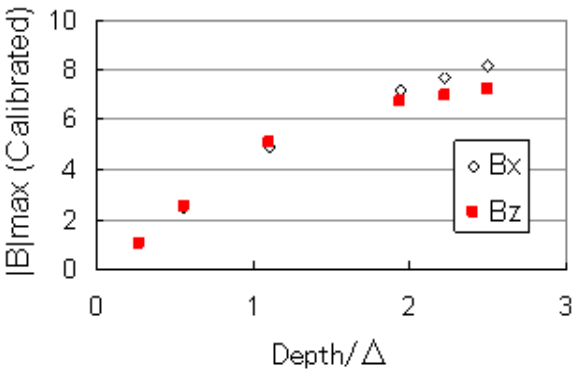

Fig. 8 Change of magnetic field signal with crack depth (cracks are 30mm long, 0.2mm wide)

3.2. Horizontal excitation coil and the defect-induced eddy current perturbation

The rectangular-shaped horizontal coil shown in Fig. 2 was utilized in the analysis in this sub-section. Magnetic field signals were taken by a pickup sensor installed centrally below the excitation coil. The defect-induced eddy current perturbation and the ECT signals were analyzed using the equivalent current models.

3.2.1. Eddy currents divert under and laterally of a crack

As shown in Fig. 9, the eddy currents induced by the horizontal excitation coil are perpendicular to the crack. The change of eddy currents resulted from diving under the crack can be modeled by a solenoid coil whose length and diameter are respectively relevant to crack length and depth, and the

magnitude of current in this hypothetical coil is relevant to eddy current density (Fig. 10(a)). Magnetic flux density above the hypothetical solenoid coil is measured. Fig. 10(a) shows that the magnetic field right above the solenoid coil is in the coil's longitudinal direction (X), of maximum magnitude right above the center of the solenoid coil, and decreases when the probe moves away from crack center. The **Bx** signals change directions at the crack's longitudinal ends.

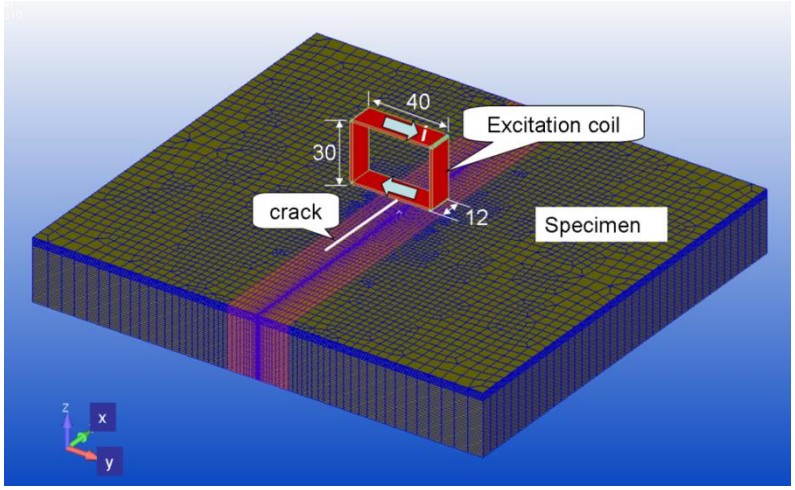

Fig. 9 Horizontal excitation coil and crack.

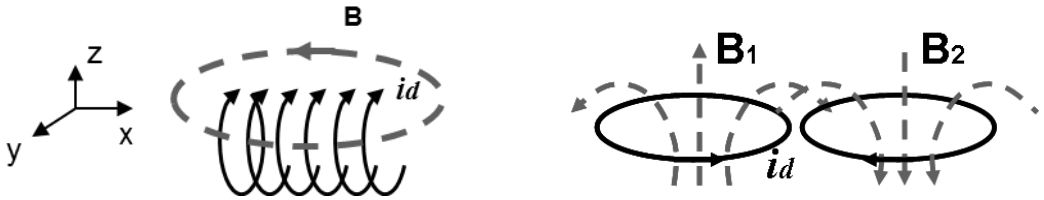

(a) solenoid coil current model **(b) elliptical current loop model**

Fig. 10 Equivalent current models to modeling the crack-induced perturbation, with a horizontal excitation coil.

On the other hand, the perturbation of eddy currents resulted from lateral bypassing is modeled by two hypothetical elliptical current loops. The correspondent ECT signal is the superimposition of magnetic fields of the two loops (Fig. 10(b)). It can be inferred that,

- When the probe is right above the crack center, the two loops with reversed currents are identical (Fig. 10(b)), and the **Bz** signal is 0.
- When the probe moves longitudinally away from crack center, the two elliptical loops whose currents are 180 degrees out of phase are no longer identical, and the **Bz** signal is nonzero. It increases with the distance from crack center, reaches maximum magnitude when the probe is over the crack's longitudinal ends where the two elliptical loops emerge into one. The **Bz** signals are longitudinally anti-symmetric about the center of a crack.

Fig. 10(b) also shows that when the probe moves longitudinally right above a crack, or along the crack's vertical centerline, **By** is always zero. The **By** signals are respectively anti-symmetric with respect to the two scan paths.

3.2.2. Verification: X, Y and Z directional signals measured by uniform eddy current probe

The equivalent current models based analysis described in sections 3.2.1 was verified by the following measurement of using a uniform eddy current probe [6].

Uniformly distributed eddy currents were induced by a horizontal excitation coil (Fig. 9) and the **X**, **Y** and **Z** directional signals were taken by a 3-axis magnetic field sensor installed centrally right

below the excitation coil. Fig. 11 shows the C-Scan of the respective directional ECT signals of a fatigue crack. Signals change their amplitudes and phases following the equivalent current models based qualitative analysis in sub-section 3.2.1. By the way, comparing to conventional pickup coil which only takes one directional signals, more comprehensive information can be acquired by this 3-axis sensor probe.

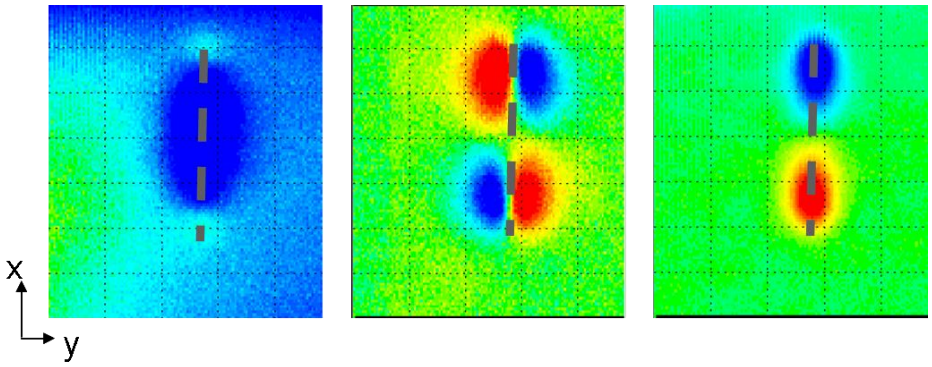

(a) X directional signal (b) Y directional signal (c) Z directional signal

Fig. 11 ECT signals measured by the 3-axis sensor probe. (the gray dashed line indicates the position of defect)

3.2.3. Crack's length/depth and directional signals

Although the X, Y, and Z directional ECT signals can be interpreted respectively by using the equivalent solenoid coil and elliptical current loop models, **Bx**, **By**, and **Bz** signals coexist and each of them is the combined effects of eddy currents bypassing laterally of and under a crack. The dominate component is determined by dimension of crack, configuration of excitation coil, excitation frequency, and etc.

The relation between respective directional signals and the dimension of cracks was analyzed by using simulation signals. Cracks of different dimensions were assumed in the center of a 30mm thick and sufficiently large test piece whose relative permeability and conductivity were respectively 1 and 1MS/m. The 40mmX30mmX12mm uniform eddy current probe depicted in Fig. 9 was assumed to scan over the cracks. The bottom surface of the excitation coil was 10mm above the test piece. The excitation frequency is 20kHz and the skin depth is 3.56mm.

Bx, and **Bz** signals (taken at a point below the center of the excitation coil, 1mm above the test piece) of cracks of various depths and lengths were calculated by FEM numerical simulation. The 0.2mm wide, 5mm long, 1mm deep crack's **Bx** and **Bz** signals' maximum amplitudes were respectively set to 1, and the signals of other cracks were calibrated accordingly. Fig.12 (a) shows the calibrated magnitude of **Bx** and **Bz** signals of cracks with various length (5, 10, 15, and 20mm, while the depth (4mm) and width (0.2mm) are fixed). Obviously the **Bx** signal is not in monotonic relation with crack length: The **Bx** signal increases with length when the cracks are shorter than 10mm, but decreases even with longer cracks. It is noticed in Fig. 9 that the excitation coil's 12mm long side is in the crack's longitudinal direction (X direction), and the length '10mm' corresponds to the excitation coil's 12mm long side. The non-monotonic relation between **Bx** signal and crack length indicates that **Bx** signal, which is mainly resulted from the bypassing of eddy currents under a crack, is inappropriate for length sizing. However, although tends to saturate when the crack is longer than the excitation coil's side length, the **Bz** signal increases monotonically with crack length, and is considered to be more appropriate for length sizing.

Fig. 12(b) shows the calibrated peak **Bx** and **Bz** signals of 15mm long, 0.2mm wide cracks of different depths. Both the **Bx** and **Bz** signals increase with crack depth, however, the **Bx** signal, which is resulted from the bypassing of eddy currents under a crack, is less likely to saturate than **Bz**, therefore is considered to be more appropriate for depth sizing.

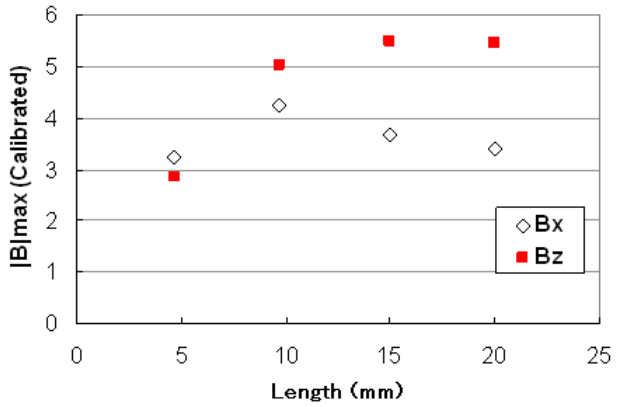

(a) Change of the maximum amplitudes of Bz and Bx signals with crack length.

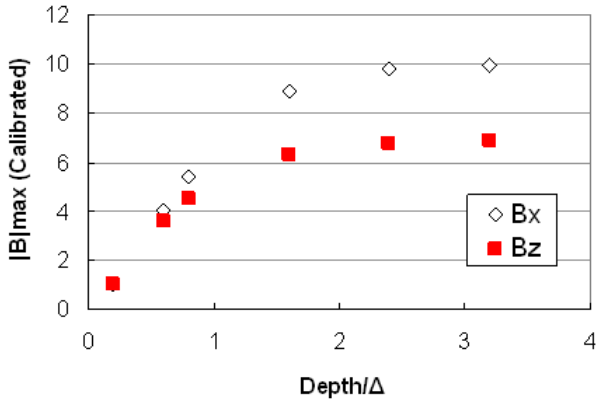

(b) Change of the maximum amplitudes of Bz and Bx signals with crack depth.

Fig. 12 Change of maximum amplitude of Bx and Bz signals with crack length and depth.

4. Crack sizing by using respective and combination of directional signals

The analysis in section 3 shows that **Bz** and **Bx** signals are relevant to crack length and depth, respectively. In this section, the respective and the combination of signals are utilized in depth sizing.

The similarity-based method (SBM) [7, 8], a non-parametric characterization approach based on multi-dimensional interpolation, was applied to depth sizing in this study. In terms of this approach, a training database consisting of a vector made of multidimensional characteristic features of cracks, $X_{tr,}$ and a vector of correspondent crack depth & length, $Y_{tr,}$ are constructed beforehand, and the required crack depth & length, $Y_{est,}$ are to be estimated from a vector of characteristic features obtained from observation signals, $X_{est,}$ by using the SBM approach.

With the arrangement shown in Fig. 9, the probe was assumed to scan longitudinally from X = -20mm to X=20mm over a set of cracks of different dimensions (the cracks were assumed to be centered at X=0). The **Bx** and **Bz** signals were obtained by numerical simulation. Fig. 13 shows the **Bx** and **Bz** signals of a 3mm deep, 8mm long semielliptical crack. The maximum amplitude (g_{max}), the correspondent phase angle (p_{max}), the location of maximum amplitude (i_{max}), and the locations where the signals reverse (i_{t1}, i_{t2}) were taken from the **Bx** signals and a characteristic feature $feat_x$ was constructed

$$feat_x = [g_{\max}, p_{\max}, i_{\max}, it_1, it_2].$$

As shown in Fig. 13(b), there are two peaks in **Bz** signals. The amplitudes of the two peaks

(g_{m1}, g_{m2}), the correspondent phase angles ($p_{m1}, p_{m2)}$ and locations (i_{p1}, i_{p2}) , the peak-to-peak value (g_{pp}) and the phase angle (ph_{pp}) were taken to construct the characteristic feature $feat_z$,

$$feat_z = [g_{m1}, p_{m1}, g_{m2}, p_{m2}, g_{pp}, ph_{pp}, ip_1, ip_2].$$

On condition that only the **Bx** signals are utilized, the training input vector X_{tr} is

$$X_{tr} = [g_{\max i}, p_{\max i}, i_{\max i}, lg_i] \qquad i = 1,2,..,N$$

where N is the number of cracks in the training set, and lg is a characteristic parameter obtained from i_{t1} and i_{t2}. In terms of **Bz** signals,

$$X_{tr} = [g_{m1i}, p_{m1i}, g_{ppi}, p_{ppi}, l_{ppi}], \qquad i = 1,2,...,N$$

where l_{pp} is a characteristic parameter obtained from locations i_{p1} and $i_{p2.}$ of the two peak. If both **B**x and **Bz** signals are utilized,

$$X_{tr} = [g_{\max i}, p_{\max i}, \lg_i, g_{m1i}, p_{m1i}, g_{ppi}, p_{ppi}], \quad i = 1,2,...,N$$

The correspondent output vector is

$$Y_{tr} = [depth_i, length_i]; \qquad i = 1,2,...,N$$

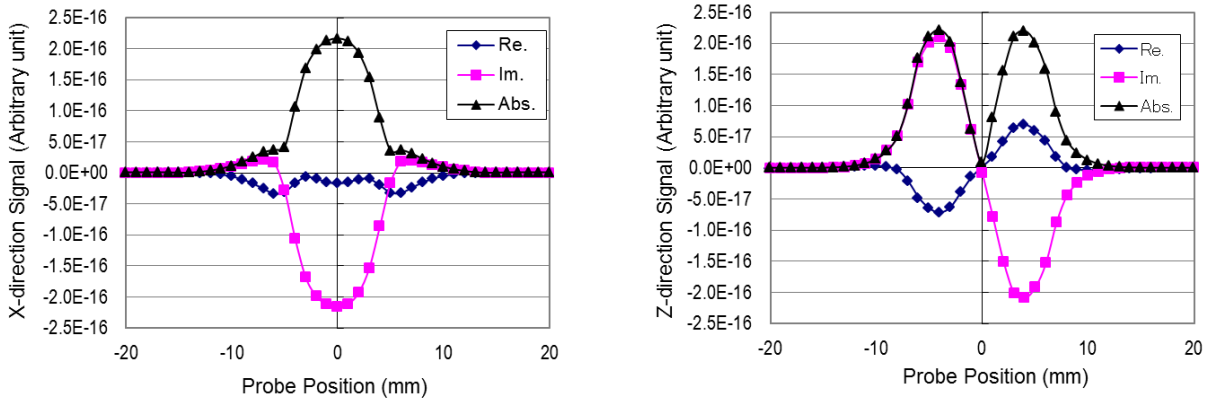

(a) Bx signals of a semielliptical crack **(b) Bz signals of a semielliptical crack**

Fig. 13 Bx and Bz signals of a semielliptical crack, taken by uniform eddy current probe. (Re.: real component, Im: imaginary component, Abs: amplitude)

In this study, 87 cracks of various lengths (2mm to 16mm), depths (0.5mm to 6mm) and shapes were assumed in a 10mm thick and sufficiently large specimen, their **Bx** and **Bz** signals were calculated by simulation and the respective characteristic features were constructed in prior. 82 of the cracks were selected randomly for training, and the remaining 5 for sizing and evaluation. This process was repeated four times, therefore totally 20 cracks were sized and evaluated. Fig. 14 shows the depth sizing results by using respectively the **Bx**, the **Bz** signals and the combination of **Bx** and **Bz** signals. Because the SBM method is a method based on 'similarity' and the selection of 'similarity coefficient', in some occasions out of range sizing results, such as crack deeper than the specimen's thickness or of negative value, appear. However, out of range estimation didn't happen when both the **Bx** and **Bz** signals were applied. For the out of range estimation, in Fig. 14, the estimated depth larger than the test piece's thickness was set as 7mm, which is even larger than the maximum crack depth (6mm) in the database, and the negative valued estimation was set as 0. The average deviation of the true and estimated crack depth under each sizing condition was calculated. The average deviation was 2.5mm of using **Bz**, the signal mainly resulted from the bypassing of eddy currents to the cracks' side surfaces, 1.2mm by using **Bx**, the signal mainly resulted from the bypassing of eddy currents under crack. The deviation was further reduced to 0.6mm when both the **Bx** and **Bz** signals were utilized.

The depth sizing results demonstrate that the ECT signals resulted from diversion of eddy currents to crack bottom are more appropriate for depth sizing. By the way, sizing accuracy and reliability can be further improved by using the combination of multi-directional signals.

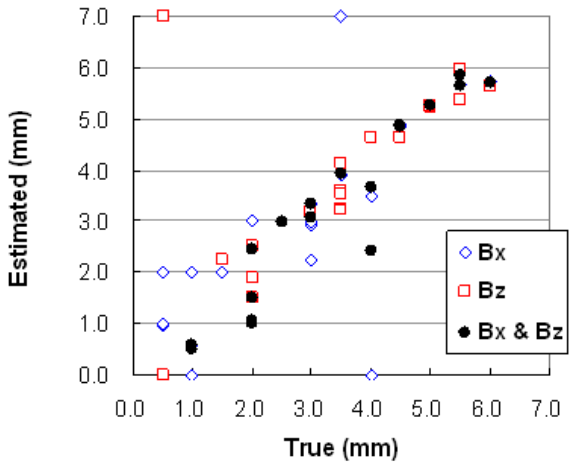

Fig. 14 Depth sizing by using Bx , Bz and the combination of Bx and Bx signals.

5. Conclusion

In this study, eddy current testing was analyzed in the view of the distribution of eddy currents and magnetic fields. The defect-induced eddy current perturbation was modeled by solenoid current coil and elliptical current loop models. The magnetic field component signals were qualitatively analyzed by the equivalent current models, and verified by ECT measurements. The study shows that

- the equivalent current models are appropriate for qualitative ECT analysis
- the sizing abilities of the respective directional field signals are different. The signals resulted from the bypassing of eddy currents under a crack are appropriate for depth sizing, and the signals resulted from the bypassing of eddy currents to crack's longitudinal ends are appropriate for crack length evaluation.
- defect sizing ability can be even enhanced by using the combination of multi-dimensional signals.

References

[1] Robert C. McMaster, Paul McIntire, and Michael L. Mester: “Nondestructive Testing Handbook”, Vol.4, Electromagnetic Testing, 2nd edition (1986).

[2] David L. Atherton: “Remote Field Eddy Current Inspection”, IEEE Trans. Magnetics, Vol. 31, No. 6, pp. 4142-4147(1995).

[3] NVE Corporation: ” GMR Sensor Catalog”, http://www.nve.com/Downloads/catalog.pdf (Accessed Dec. 20, 2014).

[4] Teodor Dogaru and Stuart T. Smith: “Giant Magnetoresistance-Based Eddy Current Sensor”, IEEE, Trans. Magnetics, Vol. 37, No. 5, pp. 3831-3838 (2001).

[5] Zhiwei Zeng, Yiming Deng, Xin Liu, Udpa L, Udpa. SS: “EC-GMR Data Analysis for Inspection of Multilayer Airframe Structures”, IEEE Trans. Magnetics, Vol. 47, No. 12, pp. 4745-4752 (2011).

[6] Kiyoshi Koyama, Hiroshi Hoshikawa, Noriyuki Taniyama: “Investigation of Eddy Current testing of Weld Zone by Uniform Eddy Current Probe”, http://www.ndt.net/article/wcndt00/papers/idn046/idn046.htm (Accessed on Oct. 09, 2013).

[7] Stephan WEGERICH: ”Condition Based Monitoring using Nonparametric Similarity Based Modeling", Proceeding of the 3rd Conference of Japan Society of Maintenology, pp.308－313 (2006).

[8] Weiying Cheng, I. Komura: “Simulation of transient eddy-current measurement for the Characterization of depth and conductivity of a conductive plate”, IEEE Trans. Magnetics, Vol. 44, No. 11, pp. 3281-3284 (2008).